Published in final edited form as:
Cell. 2007 September 7; 130(5): 837–850.

Septins Regulate Actin Organization and Cell Cycle Arrest Through SOCS7-Mediated Nuclear Accumulation of NCK

Brandon E. Kremer, **Laura A. Adang**, and **Ian G. Macara**
Dept. of Microbiology, University of Virginia School of Medicine, Charlottesville VA 22908-0577, U.S.A.

SUMMARY

Mammalian septins are GTP-binding proteins the functions of which are not well understood. Knockdown of Sept2, 6, and 7 causes stress fibers to disintegrate and the cells to lose polarity. We now show that this phenotype is induced by nuclear accumulation of the adapter protein NCK, as the effects can be reversed or induced by cytoplasmic or nuclear NCK, respectively. NCK is carried into the nucleus by SOCS7 (Suppressor Of Cytokine Signaling-7), which contains nuclear import/export signals. SOCS7 interacts through distinct domains with septins and NCK. DNA damage induces actin and septin rearrangement and rapid nuclear accumulation of NCK and SOCS7. Moreover, NCK expression is essential for cell-cycle arrest. The septin-SOCS7-NCK axis intersects with the canonical DNA damage cascade downstream of ATM/ATR and is essential for p53 Ser15 phosphorylation. These data illuminate an unanticipated connection between septins, SOCS7, NCK signaling, and the DNA damage response.

INTRODUCTION

Since their initial discovery in budding yeast, septins have been identified in all eukaryotes except plants (Longtine et al., 1996; Spiliotis and Nelson, 2006). However, the functions of these proteins in higher organisms remain unclear. There are thirteen mammalian septins, as well as multiple splice variants (Hall et al., 2005). Some are expressed ubiquitously while others are restricted to specific tissues and to post-mitotic cells (Hall et al., 2005). As in yeast, the mammalian septins have been implicated in mitosis and cytokinesis, although their mechanism is unclear (Kinoshita et al., 1997; Longtine et al., 1996; Spiliotis et al., 2005). In addition, septins are essential for sperm morphogenesis (Ihara et al., 2005; Kissel et al., 2005); others are expressed predominantly in the brain, where they may be involved in regulated exocytosis (Spiliotis and Nelson, 2006; Xue et al., 2004).

Yeast septins are better understood. They organize into a ring at the emerging bud neck and are required for proper cell division (Reviewed in (Longtine et al., 1996; Spiliotis and Nelson, 2006)). The septin ring also is a key element in morphogenetic checkpoints that respond to DNA damage (Enserink et al., 2006; Smolka et al., 2006) and to perturbations in the actin cytoskeleton (Kadota et al., 2004; Keaton and Lew, 2006). Additionally, septins function in the mitotic exit checkpoint as a scaffold for a microtubule sensor (Castillon et al., 2003; Kusch et al., 2002). Thus, septins may coordinate microtubule and actin functions during cell division and DNA damage-induced arrest in yeast.

Correspondence to: Ian Macara, Ctr. For Cell Signaling, HSC, Box 800577, Hospital West, University of Virginia, Charlottesville VA 22908-0577, Tel: 434-982-0083, Fax: 434-924-1236, Email: igm9c@virginia.edu.

Mammalian septins may also coordinate microtubule and actin dynamics. Sept2 and 9 co-localize with microtubules (Spiliotis et al., 2005; Surka et al., 2002; Vega and Hsu, 2003), and Sept2, 6, and 7 form a heteromeric oligomer that can regulate the microtubule cytoskeleton (Kremer et al., 2005; Low and Macara, 2006; Sheffield et al., 2003). The Sept2/6/7 complex associates with actin stress fibers and can be co-precipitated with anillin and actin (Joberty et al., 2001; Kinoshita et al., 2002; Kinoshita et al., 1997). Sept9 has been associated with Rho signaling and can modulate actin dynamics via an interaction with the Rho effector rhotekin and inhibition of the Rho activator SA-RhoGEF (Ito et al., 2005; Nagata and Inagaki, 2005). Furthermore, Sept9 can form trimeric complexes with Septs 7 and 11, which in turn co-localize with actin stress fibers (Nagata et al., 2004). Though a reciprocal relation between septin filaments and actin has been established, the biological relevance of interactions between mammalian septins and the actin cytoskeleton is not well understood.

We now describe a novel signaling pathway that links the Sept 2/6/7 complex to actin organization and cell morphology. The septins act through the signaling protein SOCS7 to restrict the nuclear accumulation of the adapter protein NCK, which is involved in the coordination of receptor tyrosine kinases, focal adhesions, and the actin cytoskeleton (reviewed in (Buday et al., 2002)). In the absence of septin filaments, SOCS7 recruits NCK into the nucleus. Moreover, depletion of NCK from the cytoplasm triggers the dissolution of actin stress fibers and loss of cell polarity.

We have also discovered that the association between septins, SOCS7, and NCK plays a role in the DNA damage checkpoint response. NCK rapidly and efficiently enters the nucleus following DNA damage and is necessary for UV-induced cell-cycle arrest. Furthermore, nuclear NCK is essential for activation of the tumor suppressor p53 in response to UV-induced DNA damage. Thus, we have identified a novel link between mammalian septins and actin via the SOCS7/NCK signaling pathway that couples the regulation of the DNA damage response to the cytoskeleton.

RESULTS

Silencing of septins 2, 6 and 7 causes actin cytoskeleton remodeling and changes in cell shape

To characterize the role of mammalian septins in actin organization, we targeted thee septins (Sept2, Sept6, and Sept7) that form a heteromeric complex *in vivo* and *in vitro* (Joberty et al., 2001; Low and Macara, 2006; Sheffield et al., 2003). The expression of these septins is coupled, so that a reduction in any one of them causes a decrease in the expression of the other two (Kinoshita et al., 2002; Kremer et al., 2005). We previously generated a set of siRNAs that efficiently silence Sept2, 6, and 7 in HeLa cells (Kremer et al., 2005). Septin depletion grossly affected the actin cytoskeleton and cellular morphology (Fig 1A and S1A). In control cells, the actin stress fibers were clearly visible and aligned with the long axis of the cell. By contrast, the septin-depleted cells were unpolarized, and actin was present as small fibrils throughout the cell. Any remaining stress fibers lost direction and formed disordered clusters. Similar results were observed following septin depletion in Ref52 and CHO cell lines (data not shown). As an objective measure of cellular morphology, we calculated the mean “shape factor”, $4\pi A/P^2$, where A is the cell area and P the perimeter. Shape factor values vary between 1 (perfect circle), and 0 (straight line). As shown in Fig 1B and S1B, septin knockdown significantly increased the shape factor of the cells.

To further examine the septin regulation of the actin cytoskeleton, we tested the ability of septin-depleted cells to spread on a fibronectin-coated surface, a process mediated by focal complexes and actin (Reviewed in (Martin et al., 2002)). Control- and septin-depleted cells were replated onto fibronectin-coated surfaces, fixed at various time-points, and the cellular

areas were measured. At t=5 min, septin-depleted cells were the same size as control-transfected cells (Fig 1C, D). However, septin-siRNA transfected cells spread more rapidly than control cells; after 30 min, the septin-depleted cells were significantly larger than control cells (Fig 1C, D) and had significantly more focal complexes (data not shown). Together, these results show that septins 2, 6 and 7 are required for normal organization of the actin cytoskeleton and for actin-dependent processes such as cell spreading on extracellular matrix.

Septins restrict NCK to the cytoplasm

To determine how septins regulate the actin cytoskeleton, we screened septin-depleted cells for the relocalization of proteins that may impact actin dynamics. Interestingly, the adapter protein NCK accumulated in the nuclei of septin-depleted cells (Fig 2A, B). NCK has two isoforms, both of which contain 3 SH3 domains and an SH2 domain and no classical nuclear localization signal (NLS). NCK functions in signal transduction from tyrosine kinases to the actin cytoskeleton (reviewed in (Buday et al., 2002)).

In control cells, NCK was almost exclusively cytoplasmic (Fig 2B). By contrast, NCK accumulated in the nuclei of virtually all septin-depleted cells. Immunoblots of lysates from NCK-depleted and NCK-over-expressing cells verified that our antibodies were specific and recognized both isoforms of NCK (Fig S2A, B). In addition, myc-tagged NCK1 was cytoplasmic when expressed in control cells, but became diffuse throughout the cytoplasm and nucleus in septin-depleted cells (Fig 3D). Importantly, this relocalization was specific to NCK. The distribution of the adapter protein p^{130Cas} was unchanged by septin-siRNA transfection (Fig S2C), even though NCK can bind to p^{130Cas} (Zhu et al., 1998). Thus, septin depletion induces a selective redistribution of NCK to the nucleus.

NCK is required for actin re-organization in response to septin depletion

The redistribution of NCK to the nucleus might mediate the septin knockdown phenotype or simply be an epiphenomenon. To distinguish between these possibilities, we transfected cells simultaneously with siRNAs against Sept7, NCK1, and NCK2. Knockdown efficiency was similar in all cases (Fig 2C). Those cells depleted only of NCK were long and polar, with actin stress fibers aligned along the long axis of the cell, as in control cells. Therefore, the absence of NCK is not sufficient to induce actin reorganization. Cells depleted only of septins were flat and round, as described above (Fig 2D, E). Importantly, however, cells reverted to a normal morphology when simultaneously depleted of septins and NCK (Fig 2D, E). These cells had a lower shape factor value and contained visible actin stress fibers with normal distribution. We conclude that NCK expression is required for cells to respond to loss of septins and is in a pathway downstream of or parallel to the septin-actin axis.

We next asked whether NCK is sequestered in the cytoplasm or instead shuttles constitutively in and out of the nucleus. HeLa cells were treated for 1 h with Leptomycin B (LMB), a specific inhibitor of Crm1-mediated nuclear export (Kudo et al., 1999). NCK rapidly accumulated in the nucleus after exposure to LMB (Fig S2D, E). Therefore, we conclude that endogenous NCK constitutively shuttles between the cytoplasmic and nuclear compartments, and that septins regulate the dynamics of this process.

Nuclear accumulation of NCK drives actin re-organization

We next asked whether the redistribution of NCK to the nucleus drives the loss of stress fiber integrity. To address this, we created a fusion of myc-NCK1 with a nuclear export signal (NES) to maintain myc-NCK1 in the cytoplasm. We transfected cells with control or anti-septin siRNAs, then co-transfected them with NES-NCK1 or, as a control, with myc-GFP-GFP-RanBP1 (GGBP1), a shuttling protein that is cytoplasmic at steady-state (Richards et al.,

1996). The cells were stained for the myc epitope to identify transfected cells (Fig 3A), as well as for Sept2 to verify knockdown efficiency (data not shown).

In both the control and septin-depleted cells, GGBP1 remained in the cytoplasm, proving that the relocalization of endogenous NCK was not due to a global failure of nucleocytoplasmic trafficking. The expression of GGBP1 did not affect the actin cytoskeleton or cell shape (Fig 3A, E). Importantly, however, the constitutively cytoplasmic NES-NCK1 reversed the morphological phenotype induced by septin depletion (Fig 3A, E). Additionally, on fibronectin-coated surfaces, septin-depleted cells that expressed the NES-NCK1 fusion no longer spread as rapidly as septin-depleted cells that expressed GGBP1, and were indistinguishable in size from wild type (Fig 3B, C). Thus, the ectopic expression of a constitutively cytoplasmic NCK can reverse the loss-of-septins phenotype, even though endogenous NCK presumably still accumulates in the nucleus. This result argues that the loss of NCK from the cytoplasm is responsible for the effects of septin depletion on the actin cytoskeleton.

To confirm this conclusion, we expressed myc-tagged NCK without an NES. This construct distributed diffusely throughout the cell, both within the nucleus and in the cytoplasm. Nonetheless, it reversed the cell-rounding phenotype (Fig 3D, E), supporting the idea that cell rounding is caused by depletion of NCK from the cytoplasm, rather than through any specific action of NCK within the nucleus.

How can these data be reconciled with our observation that silencing of NCK expression does not disrupt the actin cytoskeleton? One possibility is that the effect is indirect – that nuclear NCK sequesters a binding partner and that the loss of this partner from the cytoplasm causes cell rounding. To test this hypothesis, we expressed a constitutively nuclear NLS-NCK1 fusion protein. Strikingly, the transfected cells lost their polar orientation and became more circular. Moreover, the actin stress fibers dissolved into small, curled filaments, as occurs after septin depletion (Fig 3D, E). Therefore, the forced expression of nuclear NCK phenocopied the effects of septin depletion, while elevated cytoplasmic NCK reversed the effects. We conclude that nuclear NCK sequesters an effector that normally acts in the cytoplasm to maintain actin stress fibers and polarized cell morphology.

SOCS7 mediates the nuclear transport of NCK

NCK contains no classical NLS or NES. We hypothesized, therefore, that NCK is transported through the nuclear pores by association with an adapter protein. One NCK-binding protein, Suppressor Of Cytokine Signaling 7 (SOCS7), contains both an N-terminal leucine-rich region, postulated to be a NES, as well as a central basic region with homology to a classical monopartite NLS. In addition to the predicted full-length protein, two naturally occurring splice variants of SOCS7, lacking either the NCK binding domain (SOCS7 ΔNBD) or the NES (NAP4), have been described (Martens et al., 2004; Matuoka et al., 1997) (Fig S3A).

To verify that SOCS7 binds to NCK, as previously reported (Martens et al., 2004; Matuoka et al., 1997), we expressed myc-tagged NAP4, SOCS7 ΔNBD, or full-length SOCS7 in 293T cells, immunoprecipitated with anti-myc, and probed for co-precipitation of endogenous NCK, The NAP4 and full-length SOCS7, but not SOCS7 ΔNBD, co-precipitated specifically with endogenous NCK (Fig S3B). We next verified the functionality of the nuclear traffic signals. Myc-tagged SOCS7 localized to the cytoplasm, while LMB treatment caused the SOCS7 to accumulate in the nucleus (Fig S3C), consistent with sequence information that SOCS7 contains a Crm1-dependent NES. In contrast, myc-NAP4, which contains the putative NLS but lacks the N-terminal NES, was exclusively nuclear. Next, we bound the nuclear import factor Impα3 to beads and added cell lysate containing myc-SOCS7. The myc-SOCS7

specifically co-precipitated with Impα, demonstrating that SOCS7 contains a *bona fide* NLS (Fig S3D).

To determine whether SOCS7 is the nuclear import factor for NCK, we silenced expression of SOCS7 by RNAi, then treated control- or SOCS7-depleted cells with LMB and stained for endogenous NCK. As predicted, NCK accumulated in the nuclei of control-transfected cells after LMB treatment, but SOCS7 depletion greatly reduced the fraction of cells with nuclear NCK (Fig S3E, F). Therefore, NCK requires SOCS7 for nuclear import.

SOCS7 binds to septins and responds to septin depletion

These results raised the possibility that SOCS7 couples septins to NCK localization. To investigate this idea, we generated antibodies against SOCS7, then immunoprecipitated Sept6 and assayed for co-precipitation of endogenous SOCS7. Sept6 specifically co-precipitated a double band that was detected by the anti-SOCS7 antibody (Fig 4A, Top). However, at 120–140 kDa, this band was larger than the previously reported size of SOCS7. Therefore, we repeated the co-precipitation in cells transfected with siRNAs against SOCS7. The siRNAs reduced the intensity of the double band by >80% (Fig 4A, Bottom), and we conclude that HeLa cells express an unusually long splice variant of SOCS7. Only the shorter SOCS7 variants have been previously characterized, however, (Martens et al., 2004;Matuoka et al., 1997) so these were used in our further experiments.

To identify the specific region of SOCS7 bound by septins, myc-NAP4 or -SOCS7 were expressed in HEK 293T cells and assayed for binding to endogenous Sept6. As shown in Fig 4B, full-length SOCS7, but not NAP4, co-precipitated specifically with the septin complex, suggesting that the N-terminal domain of SOCS7 contains the septin binding site. Additionally, the isolated N-terminus of SOCS7 fused to GFP (GFP-SOCS7(1-124))co-precipitated with the septin complex (Fig 4C). Thus, the N-terminal domain, which contains the NES, is both necessary and sufficient for septin association. Of note, GFP-NCK did not co-precipitate with Sept6 (Fig 4C).

We next asked if septins regulate SOCS7 localization. In control cells, full-length myc-SOCS7 was predominantly cytoplasmic. However, SOCS7 was no longer excluded from the nucleus following septin depletion (Fig 4C, D). To determine whether the relocalization is dependent on NCK binding, we transfected cells with a splice variant of SOCS7 that lacks the NCK binding domain (ΔNBD). The distribution of this deletion mutant was indistinguishable from wild type, both in control cells and in cells depleted of septins (Fig 4C). Moreover, the ΔNBD mutant accumulated in the nucleus in response to LMB treatment (Fig S3B). We conclude that SOCS7 localization is dependent on septins, and NCK import requires SOCS7, but SOCS7 import is independent of NCK binding.

SOCS7 is necessary for septin regulation of NCK and actin organization

If SOCS7 is a key component of the septin-NCK-actin pathway, then its absence should block the effects of septin knockdown on both cell morphology/actin organization and NCK localization. To test this prediction, we knocked down SOCS7 and/or septins and examined the morphological response (Fig 5A). Control and SOCS7-depleted cells were long and polar, with well-organized actin stress fibers (Fig 5B, C). As expected, cells lacking septins were large and circular, with disordered actin. Importantly, however, cells depleted of both Sept7 and SOCS7 were indistinguishable from control-transfected cells (Fig 5B, C), demonstrating that the septin depletion phenotype is dependent on SOCS7 expression.

We next stained the siRNA-transfected cells for endogenous NCK (Fig 5D). In control cells, the NCK was mostly cytoplasmic, and SOCS7 depletion resulted in a small increase in the

cytoplasmic/nuclear ratio (Fig 5D, E), consistent with our finding that SOCS7 is the major import factor for NCK. However, although NCK accumulated in the nuclei of septin-depleted cells, in the double-knockdown cells it remained cytoplasmic (Fig 5D, E). Thus, SOCS7 links septins to NCK localization.

Nuclear NCK is Necessary for DNA Damage-Induced Cell Cycle Arrest

A key question concerns the biological function of NCK relocalization to the nucleus. Endogenous NCK is occasionally present in the nuclei of control cells (Fig 2B), hinting that its localization might be somehow linked to the cell cycle. Moreover, the Sept2/6/7 complex reorganizes during cell division (Kinoshita et al., 1997;Oegema et al., 2000;Spiliotis et al., 2005), and we wondered whether septin depletion mimics this reorganization. To test this idea a GFP-NCK1 fusion was expressed at low levels in HeLa cells, and confocal images were collected at intervals over a period of ~8 h. However, under conditions where phototoxicity was minimized, the GFP-NCK remained exclusively cytoplasmic until nuclear envelope breakdown (Supplemental Movie 1). In contrast, at higher levels of illumination (i.e., irradiation), the GFP-NCK frequently accumulated within nuclei, but after several hours the cells died (Supplementary Movie 2). This outcome suggested that NCK might be involved in the DNA damage response.

To explore this possibility, we subjected HeLa cells to a variety of genotoxic stresses, including UV irradiation, hydroxyurea, and mitomycin C, and stained the cells for endogenous NCK. We also treated cells with thymidine, which activates the ATM, Chk1, and Chk2 checkpoint kinases without actually causing DNA damage (Bolderson et al., 2004). Remarkably, all of these treatments resulted in the redistribution of NCK to the nucleus (Fig 6A, B and Fig S4A, B). Moreover, nuclear accumulation was rapid, occurring within 1 h of exposure to UV radiation, and was accompanied by an increase in shape factor values (Fig S4C). Conversely, more general stressors, including heat shock and Cytochalasin D, had no effect on NCK localization (data not shown).

To assess whether NCK is required for the DNA damage checkpoint response, we used wild-type mouse embryonic fibroblasts (NCK^{wt}) and fibroblasts derived from NCK1−/− NCK2−/− embryos (NCK−/−) (Bladt et al., 2003) and counted cell numbers 0 and 24 h after irradiation (Fig 6C). Whereas NCK^{wt} cells were unable to proliferate following UV irradiation (Fig 6C, filled triangles), NCK−/− cells continued to grow (Fig 6C, filled circles). Next, we compared NCK^{wt} with NCK−/− cells by propidium iodide (PI) DNA content analysis. Checkpoint induction or delayed progression through a particular phase of the cell cycle would result in an accumulation of cells in that phase. NCK−/− cells had a lower background percentage of cells in G1 than did the wild type cells (Fig 6D). In response to UV-induced DNA damage, the NCK^{wt} cells accumulated in G1 and G2, as predicted (≥6 trials/condition) and showed an increased percentage of sub-G1 cells (presumptively apoptotic cells) (Fig 6D). Strikingly, however, the NCK−/− cells were not susceptible to UV-induced cell cycle arrest (5 trials/condition).

To verify that the failure to arrest was caused by the absence of NCK, we asked if the re-introduction of NCK1 and NCK2 into the knockout cells would re-sensitize them to UV radiation. Cells were costained with PI and mouse anti-myc, and the myc-expressing cells were selected for analysis. The over-expression of myc-NCK in NCK−/− cells significantly increased the fraction of cells in G1 (Fig 6D). This effect was not due to the transfection itself, as ungated cells within the same population did not exhibit significantly different cell cycle profiles compared to untransfected NCK^{-} cells (Transfected cells: G1 = 51.0% ± 4.5%. Total cells: G1 = 35.9% ± 1.5%). Next, we asked whether NCK over-expression would reverse the NCK knockout phenotype. Indeed, following UV irradiation, the NCK−/− cells transfected with NCK1 and NCK2 arrested efficiently in G1 and G2 (Fig 6D) (3 trials/condition). In

addition, NCK expression restored UV sensitivity to NCK−/− cells in a cell proliferation assay (Fig S4D). We conclude, therefore, that NCK expression slows progression through G1 and is essential for DNA damage-induced cell cycle arrest.

Since SOCS7 is the major transport factor for NCK, we next investigated if SOCS7 relocalizes to the nucleus after UV irradiation. HeLa cells were UV-irradiated and fixed after 1h, and the cells were stained for endogenous SOCS7. As shown in Fig 6E and Fig S4E, UV irradiation caused a rapid relocalization of SOCS7 into the nucleus.

Next, HeLa cells were UV-irradiated then fixed at various time points and stained for filamentous actin and Sept2. Intriguingly, UV irradiation induced many of the same changes that we observe after septin knockdown (Fig 6F). Within 1 h, the cells lost many of their stress fibers and began to assume a circular morphology. After 2 h, virtually all cells had lost polarity, and the actin cytoskeleton was almost entirely dissolved into small, curved filaments. In addition, the architecture of the septin cytoskeleton was dramatically altered; the clear actin-associated filaments visible in untreated cells virtually disappeared after 2 h. Similar results were observed following treatment with hydroxyurea (data not shown). These data suggested a hitherto unsuspected link between mammalian septins, the actin cytoskeleton, and the DNA damage response checkpoint.

Nuclear Transport of NCK is Necessary for Activation of p53

To further explore the link between DNA damage and the actin cytoskeleton, we examined the role of NCK in the canonical DNA damage pathway. First, HeLa cells were transfected with control- or anti-NCK siRNAs, then UV-irradiated, and the effects of NCK depletion on Chk2 activation were assayed (Fig 7A). We observed that the phosphorylated Chk2 on Th68 was decreased by ~50% in NCK-depleted cells. In addition, the level of Chk2 protein was reproducibly reduced in NCK-depleted cells, though the loss of phosphorylation was greater than the loss of total Chk2.

Next, WT and NCK^{-} MEFs were subjected to UV irradiation and probed for activation of ATM, ATR, and p53 (Fig 7B). The NCK-deficient MEFs were able to efficiently activate ATM and ATR in response to UV-irradiation. Strikingly, however, the NCK^{-} cells were unable to phosphorylate p53 at Ser15 following DNA damage. The levels of phosphorylated p53 were drastically reduced (>90%) in NCK−/− cells as compared to WT MEFs and were indistinguishable from non-irradiated cells. These data together indicate that NCK is not necessary for the detection of DNA damage by ATM/ATR but is essential for efficient activation of downstream effectors of the DNA damage response. To examine Chk2 levels in the mouse cells we stained control- and UV-irradiated WT and NCK−/− MEFs for phospho-Chk2 (T68) and total Chk2 and analyzed activation within individual cells by flow cytometry. UV-irradiation of WT cells induced a 2-fold increase in Chk2 mean fluorescent intensity (MFI), normalized for total Chk2 protein (Fig. 7C). Two distinct populations were seen: a large population in which MFI increased by 3.3-fold (+/− 0.2, SEM, n=4), and a smaller population lacking Th68 phosphorylated Chk2. NCK^{-} cells, however, were unable to efficiently phosphorylate Chk2: the overall MFI increased by only 1.4-fold, 30% ± 5% (SEM) less than in WT cells. These data are consistent with the results observed in HeLa cells (Fig 7A).

The results described above show that NCK interacts with the DNA damage pathway between detection (ATM/ATR) and effectors (Chk2/p53). We next asked whether the transport of NCK into the nucleus after UV-irradiation is necessary for full activation of Chk2. As described above, NCK was predominantly cytoplasmic in non-irradiated cells and nuclear in UV-irradiated control-transfected cells. Importantly, depletion of SOCS7 blocked translocation of NCK to the nucleus in response to UV irradiation, confirming that SOCS7 is the transporter for NCK in response to DNA damage (Fig 7D and Fig S4F). SOCS7 depletion also blocked

the morphological changes induced by UV-irradiation (Fig S4G). Next, to determine whether the nuclear transport of NCK is necessary for activation of the DNA damage pathway, we transfected HeLa cells with control- or SOCS7-siRNA, then UV-irradiated the cells. SOCS7 depletion decreased Chk2 phosphorylation at T68 (Fig. 7E), with no change in NCK or Chk2 expression (Fig 7E). Thus, relocalization of NCK to the nucleus is essential for complete activation of the pathway.

Finally, we asked whether septin depletion would alter the response to DNA damage. Knockdown of either Sept2 or Sept7 in WT MEFs significantly potentiated the increase in p53 phosphorylation following UV irradiation (Fig 7F). Importantly, however, septin depletion did not increase p53 phosphorylation in the absence of UV irradiation, showing that nuclear trafficking of NCK is necessary, but not sufficient for, activation of the checkpoint pathway.

DISCUSSION

We have identified a new signaling pathway that couples septins to the actin cytoskeleton through nuclear translocation of NCK by SOCS7. Unexpectedly, this pathway is linked to the DNA damage checkpoint response. The SOCS proteins have traditionally been considered to function as negative regulators of signal transduction pathways involving cytokines, growth hormone, insulin and leptin, and SOCS7 alters the nuclear localization of activated STAT3 (Howard and Flier, 2006; Krebs and Hilton, 2000; Martens et al., 2005). We now report that SOCS7 regulates the nucleo-cytoplasmic distribution of NCK, that septins bind to SOCS7, and that this interaction is necessary to maintain both SOCS7 and NCK in the cytoplasm. Although we demonstrate direct septin-SOCS7 binding, the mechanism by which septins impact SOCS7 distribution remains unclear. Neither SOCS7 nor NCK co-stained with septin filaments, but evidence is lacking that filaments are the functional form of mammalian septins, and the key, regulatory pool of septins might be diffusely distributed through the cytoplasm. Septins bind to several kinases and phosphatases in a variety of model systems (Reviewed in (Field and Kellogg, 1999; Spiliotis and Nelson, 2006)), and it is possible that these septin-bound enzymes modify SOCS7 and maintain the cytoplasmic distribution seen at steady-state.

Previous reports have shown that loss of septins in NIH 3T3 cells perturbs actin bundles, particularly those underneath the nucleus (Kinoshita et al., 2002). These data appear to contradict observations on MEFS from septin knockout mice, in which the cell morphology and actin cytoskeleton appear unchanged (Ono et al., 2005). However, depletion of a single septin in cell lines by RNAi results in the loss of other septins within the complex (Kinoshita et al., 2002; Kremer et al., 2005), whereas deletion within embryos does not alter the expression of other septin proteins (Ono et al., 2005), possibly because of compensation or functional redundancy between septin family members.

In *S. cerevisiae*, septins are key elements in a morphogenetic checkpoint that responds to cytoskeletal perturbations, mediated through the protein kinase Swe1p (Keaton and Lew, 2006; Lew, 2003; Longtine et al., 2000). Recently, septins were reported to bind the Chk2 homologue Rad53, illuminating a link between the checkpoint response and morphology in polarized cell growth (Enserink et al., 2006; Smolka et al., 2006). There is also evidence that septins function in the mitotic exit checkpoint as a scaffold for a microtubule sensor. Thus, yeast septins and septin-dependent kinases may coordinate microtubule and actin functions in cell division (Castillon et al., 2003; Kusch et al., 2002). We now propose that vertebrate septins perform similar functions. Sept2 binds and inhibits the microtubule associated protein, MAP4 (Kremer et al., 2005); it also decorates microtubules during mitosis and might regulate the spindle assembly checkpoint (Spiliotis et al., 2005). Our present results demonstrate a link between septins, the actin cytoskeleton, and the DNA damage checkpoint response. However,

whether the septins integrate all these functions through recruitment of protein kinases, as in yeast, remains to be determined.

We propose that a complex composed of septin proteins (including Sept2,6,7) interacts with the nucleo-cytoplasmic shuttling protein SOCS7 in such a way as to maintain it predominantly in the cytoplasm at steady state. SOCS7, in turn, binds to and retains NCK in the cytoplasm. Both proteins, however, are constantly shuttling between the two compartments and, following DNA damage, SOCS7 and NCK accumulate in the nucleus. This accumulation is essential both for morphological changes and for the activation of downstream members of the DNA-damage kinase cascade. In the absence of either protein, the activation of Chk2 and p53 is inhibited, and cell cycle arrest does not occur. In the absence of septins, activation is potentiated. Nuclear accumulation of NCK is, however, insufficient to induce Chk2/p53 activation in the absence of ATM/ATR activation, which occurs only following DNA damage. Concurrently, depletion of NCK from the cytoplasm results in defects in signaling to the actin cytoskeleton and loss of cell polarity. Therefore, the spatial distribution of NCK plays a pivotal role in coupling the DNA damage checkpoint to actin dynamics. Interestingly, NCK has recently been implicated in cellular responses to endoplasmic reticulum stress, which leads to the inhibition of translation (Latreille and Larose, 2006). Thus, NCK may function as a pivotal integrator between mitogen-stimulated growth signals and a variety of stresses that inhibit cell growth and division.

EXPERIMENTAL PROCEDURES

Constructs, cell culture, and transfections

HeLa cells were grown in DMEM with 5% CS and 5% FCS. SiRNAs (Kremer et al., 2005) were purchased from Dharmacon, Inc. (LaFayette, CO) and were transfected with Oligofectamine (Invitrogen). For siRNA-DNA co-transfections, cells were first transfected with siRNA using Oligofectamine, then, after 48 h, with plasmids using FuGene6 (Roche), and grown for an additional 24 h. MEFs were grown in DMEM containing 10% FCS and transfected using Lipofectamine 2000 as described previously (Smith et al., 2005). Construction of NCK2, NES- and NLS-NCK1, and full-length SOCS7 constructs is described in Supplemental Materials.

Immunofluorescence and immunoblotting

Antibody and reagent sources are given in Supplementary Materials.

Immunofluorescence staining and immunoblots were performed as described previously (Kremer et al., 2005). Images from random fields were captured on a Nikon TE200 inverted fluorescence microscope with a 60x water immersion lens (na = 1.3) and an ORCA charge-coupled device camera (Hamamatsu, Bridgewater, NJ) controlled by Openlab 5.0 software (Improvision). Shape factor = $4\pi A/P^2$. P values were calculated by a two-tailed Student's t-test. To quantify nuclear-cytoplasmic distributions, protein staining was scored as "cytoplasmic" if the intensity was greater in the cytoplasm than in the nucleus, "nuclear" in the opposite case, or "equal" if no difference was observed between nucleus and cytoplasm.

Cell spreading assays

Cell spreading assays on fibronectin were performed as described previously (Joberty et al., 1999). Control- or septin-depleted cells were resuspended and plated onto Labtek II chamber slides that had been coated with 50 μg fibronectin (Sigma). Cells were fixed and stained as described previously (Kremer et al., 2005). Cell areas were measured by collecting random fields at 20X magnification and analyzed using Openlab software.

Immunoprecipitations

To co-immunoprecipitate septin binding partners, cells were lysed as described previously (Joberty et al., 2000). The lysate was cleared by centrifugation, and the supernatant was added to Protein A-Sepharose beads (Sigma) pre-complexed to monoclonal anti-GST or anti-Sept6 hybridoma supernatant (Kremer et al., 2005) and agitated for 1h at 4°C. The beads were washed 3X in 20 bed vols each of wash buffer (Joberty et al., 2000), then resuspended in 1 bed vol 2X SDS-PAGE buffer. For co-precipitation of expressed protein, HEK 293 cells were transfected using Lipofectamine 2000 (Invitrogen) 24h prior to lysis and immunoprecipitation.

DNA Damage and Cell cycle analysis

To induce DNA damage, growth medium containing 2 mM hydroxyurea (HU), 1 μM mitomycin C (MMC), 10 mM thymidine, or with the appropriate volume of vehicle was added to each well. For UV irradiation, cells were grown overnight, washed once in PBS, then exposed to 20 J/m^2 of UV-A radiation. The PBS was aspirated, and growth medium was added. The cells were grown for the times indicated, fixed, and stained as described above. Immunoblots were performed 1h after irradiation.

For flow cytometric analysis of UV-irradiated cells, the cells were washed twice in PBS, detached by addition of 5 mM EDTA plus 1 mM EGTA in PBS, and fixed in ice-cold 70% ethanol for at least 2h. The cells were washed 3X in PBS, and equal numbers of cells were resuspended in 500 μl Vindelov's solution (Sibani et al., 2005). Analysis was performed 29h after UV irradiation on a Becton Dickinson FACSCalibur. Fluorescence compensation and cell cycle analysis was performed using FlowJo version 6.4.2 (Tree Star) analysis package and the Jeff-Dean-Fox model (Fox, 1980). Cell cycle analysis of NCK1/2 transfected cells and chk2 staining of WT and NCK^{-} MEFs is described in Supplemental Materials.

Supplementary Experimental Procedures

Cloning

NCK2 was cloned from kidney cDNA (Invitrogen) using the primers GAAGGACTCCAGGATCCATGACAGAAGAAGTTATTGTGATAGCC and CGGGGAATTCTCACTGCAGGGCCCTGACG, digested with BamHI and EcoRI, and ligated into pK-myc. To generate NLS- and NES-tagged NCK constructs, oligos corresponding to the NES of PKI (GATCCGGCCTGGCCCTGAAGCTGGCCGGCCTGGACATCGGCG and GATCCGCCGATGTCCAGGCCGGCCAGCTTCAGGGCCAGGCCG) or to the NLS of the SV40 large T antigen (GATCCGGCCCCAAGAAGAAGCGGAAGGTGGGCG and GATCCGCCCACCTTCCGCTTCTTCTTGGGGCCG) were generated, annealed, and phosphorylated, and the resulting duplexes were ligated into the BamHI site of pK-myc-NCK1 or –NCK2. To make the full-length SOCS7 construct, a BlpI-BglII fragment of NAP4, which contains the NCK binding domain, was ligated into the SOCS7 (ΔNBD) construct that had been digested similarly and dephosphorylated. Proper insertion of the NBD was verified by sequencing.

Antibodies and other reagents

Mouse anti-NCK was from BD Transduction Labs; rabbit anti-NCK was from Tony Pawson (Univ. of Toronto, Canada). Except in Fig. S2B, all immunoblots were performed with rabbit anti-NCK, and all immunofluorescence was carried out using mouse anti-NCK.

The anti-septin antibodies have been described previously (Kremer et al., 2005). Rabbit anti p^{130Cas} was from Amy Bouton (Univ. of Virginia). Anti myc 9E10 antibody was from the University of Virginia hybridoma facility. Rabbit anti-phospho-p53 (Ser15), -phospho-ATR (Ser428), -phospho-Chk2 (Thr68), and mouse anti-phospho ATM (Ser1981) was from Cell

Signaling Technology. Mouse anti-ATR was from Genetex. Rabbit anti-ATM and anti-Chk2 was from AbCam. Mouse anti-p53 was from Calbiochem. Phalloidin was obtained from Sigma. Myc-tagged NCK1 was a kind gift of Tom Parsons (Univ. of Virginia). NCK1/NCK2 knockout MEFs were from Dr. Tony Pawson (Univ. of Toronto, Canada). A clone of human SOCS7 lacking the NCK binding domain (SOCS7 (ΔNBD)) was from P. Wang and R. Beyaert (Ghent University). The N-terminal deletion splice variant NAP4 was from K. Matuoka and R. Beyaert (Ghent University).

To generate the rabbit anti-SOCS7 antibody, a peptide corresponding to a specific C-terminal region of SOCS7 (CAQLISKQKQEVEPS) was generated (UVA Peptide Synthesis Facility) and coupled to KLH (Pierce Biochemical). Polyclonal rabbit antisera were produced (Cocalico) and affinity purified to the immunizing peptide coupled to Sulfolink beads (Pierce Biochemical) according to manufacturer's instructions.

siRNA co-transfections

In the text, "NCK siRNA" indicates that equal amounts of specific NCK1 and NCK2 dsRNA from Dharmacon were transfected into cells. For NCK-Sept7 siRNA, cells were transfected either with 100% control siRNA; 2/3 control siRNA + 1/3 Sept7 siRNA; 1/3 each control-, NCK1-, and NCK2 siRNA; or 1/3 each Sept7-, NCK1-, and NCK2 siRNA. For SOCS7-Sept7 siRNA, cells were transfected either with 100% control siRNA; 50% each control- and Sept7 siRNA; 50% each control- and SOCS7 siRNA; or 50% each Sept7- and SOCS7 siRNA.

FACS of immunostained Mouse Embryonic Fibroblasts

For cell cycle analysis of NCK1/2-transfected NCK^{-} cells, cells were transfected as described above with plasmids containing myc-NCK1 and -NCK2, incubated 24h, then UV-irratiated (20 J/m^2) as described above and incubated in medium for another 29h. The cells were lifted and fixed as described above, washed 3X in PBS, then blocked in PBS containing 4% calf serum for 20 min. The cells were permeabilized in permeabilization buffer (PB) (PBS, 4% calf serum, 0.2% saponin), washed twice in PB, then stained with primary anti-myc antibody for 1h at room temperature in PB. The cells were washed twice in PB and stained with Alexa488-conjugated donkey anti-mouse antibody (Molecular Probes) for 1h in PB. The cells were washed twice more in PB, once in PBS, then counted and resuspended in Vindelov's solution (3.4 mM Tris, pH 7.4, 75 μM propidium iodide, 0.1% NP40, 700 U/L RNase A (Sigma)). Cells were collected and fluorescence compensated as described above. Myc-NCK positive cells were selected by gating on 'high expressors' (fluorescence intensity greater than ~5×10^2; ~10% of total transfected cells) for further cell cycle analysis.

To stain phosphorylated and total Chk2 by flow cytometry, cells were lifted and fixed as described above. Cells were then permeabilized in ice-cold methanol for 3 min, then washed and blocked 15 min in PB. The samples were split into two equal volumes, and the cells were stained with anti-Chk2 (Cell Signaling Technology; 1/250) or with anti-phospho-Chk2 T68 (Cell Signaling Technology, 1/25) in PB. Cells were washed three times in PB, incubated with Alexa488-conjugated goat anti-rabbit antibody (Molecular Probes), and washed three more times before collection and fluorescence compensation as described above.

Proliferation assays of NCK-transfected cells

NCK^{WT} cells expressing GFP, NCK−/− cells expressing GFP, or NCK−/− cells expressing NCK1, NCK2 and GFP were plated, in triplicate, onto 3 separate 24-well plates (9 total wells/transfection). Twenty-four h post-transfection (t=0h), one triplicate sample for each condition was trypsinized, the number of GFP-expressing cells in each replicate was counted in duplicate, and the mean value was normalized to 100%. One 24-well plate was UV-irradiated, and both

UV− and UV+ cells were grown for an additional 24h, at which time the numbers of GFP-expressing cells in both irradiated and control samples were counted.

Supplementary Material

Refer to Web version on PubMed Central for supplementary material.

Acknowledgements

We thank the following for the generous provision of reagents: M. Schwartz, A. Bouton, and T. Parsons (Univ. of Virginia), T. Pawson (Univ. of Toronto), P. Wang, K. Matuoka, and R. Beyaert (Ghent University). This work was supported by grants GM66306 and GM50526 from the National Institutes of Health. BEK and LAA were supported in part by NIH Medical Scientist Training Grant T32 GM 07267-27.

References

Bladt F, Aippersbach E, Gelkop S, Strasser GA, Nash P, Tafuri A, Gertler FB, Pawson T. The murine Nck SH2/SH3 adaptors are important for the development of mesoderm-derived embryonic structures and for regulating the cellular actin network. Mol Cell Biol 2003;23:4586–4597. [PubMed: 12808099]

Bolderson E, Scorah J, Helleday T, Smythe C, Meuth M. ATM is required for the cellular response to thymidine induced replication fork stress. Hum Mol Genet 2004;13:2937–2945. [PubMed: 15459181]

Buday L, Wunderlich L, Tamas P. The Nck family of adapter proteins: regulators of actin cytoskeleton. Cell Signal 2002;14:723–731. [PubMed: 12034353]

Castillon GA, Adames NR, Rosello CH, Seidel HS, Longtine MS, Cooper JA, Heil-Chapdelaine RA. Septins have a dual role in controlling mitotic exit in budding yeast. Curr Biol 2003;13:654–658. [PubMed: 12699621]

Enserink JM, Smolka MB, Zhou H, Kolodner RD. Checkpoint proteins control morphogenetic events during DNA replication stress in *Saccharomyces cerevisiae*. J Cell Biol 2006;175:729–741. [PubMed: 17130284]

Field CM, Kellogg D. Septins: cytoskeletal polymers or signalling GTPases? Trends Cell Biol 1999;9:387–394. [PubMed: 10481176]

Fox MH. A model for the computer analysis of synchonous DNA distributions obtained by flow cytometry. Cytometry 1980;1:71–77. [PubMed: 7023881]

Hall PA, Jung K, Hillan KJ, Russell SE. Expression profiling the human septin gene family. J Pathol 2005;206:269–278. [PubMed: 15915442]

Howard JK, Flier JS. Attenuation of leptin and insulin signaling by SOCS proteins. Trends Endocrinol Metab 2006;17:365–371. [PubMed: 17010638]

Ihara M, Kinoshita A, Yamada S, Tanaka H, Tanigaki A, Kitano A, Goto M, Okubo K, Nishiyama H, Ogawa O, et al. Cortical organization by the septin cytoskeleton is essential for structural and mechanical integrity of mammalian spermatozoa. Dev Cell 2005;8:343–352. [PubMed: 15737930]

Ito H, Iwamoto I, Morishita R, Nozawa Y, Narumiya S, Asano T, Nagata K. Possible role of Rho/Rhotekin signaling in mammalian septin organization. Oncogene 2005;24:7064–7072. [PubMed: 16007136]

Joberty G, Perlungher RR, Macara IG. The Borgs, a new family of Cdc42 and TC10 GTPase-interacting proteins. Mol Cell Biol 1999;19:6585–6597. [PubMed: 10490598]

Joberty G, Perlungher RR, Sheffield PJ, Kinoshita M, Noda M, Haystead T, Macara IG. Borg proteins control septin organization and are negatively regulated by Cdc42. Nat Cell Biol 2001;3:861–866. [PubMed: 11584266]

Joberty G, Petersen C, Gao L, Macara IG. The cell-polarity protein Par6 links Par3 and atypical protein kinase C to Cdc42. Nat Cell Biol 2000;2:531–539. [PubMed: 10934474]

Kadota J, Yamamoto T, Yoshiuchi S, Bi E, Tanaka K. Septin ring assembly requires concerted action of polarisome components, a PAK kinase Cla4p, and the actin cytoskeleton in *Saccharomyces cerevisiae*. Mol Biol Cell 2004;15:5329–5345. [PubMed: 15371547]

Keaton MA, Lew DJ. Eavesdropping on the cytoskeleton: progress and controversy in the yeast morphogenesis checkpoint. Curr Opin Microbiol. 2006

Kinoshita M, Field CM, Coughlin ML, Straight AF, Mitchison TJ. Self- and actin-templated assembly of Mammalian septins. Dev Cell 2002;3:791–802. [PubMed: 12479805]

Kinoshita M, Kumar S, Mizoguchi A, Ide C, Kinoshita A, Haraguchi T, Hiraoka Y, Noda M. Nedd5, a mammalian septin, is a novel cytoskeletal component interacting with actin-based structures. Genes Dev 1997;11:1535–1547. [PubMed: 9203580]

Kissel H, Georgescu MM, Larisch S, Manova K, Hunnicutt GR, Steller H. The Sept4 septin locus is required for sperm terminal differentiation in mice. Dev Cell 2005;8:353–364. [PubMed: 15737931]

Krebs DL, Hilton DJ. SOCS: physiological suppressors of cytokine signaling. J Cell Sci 2000;113(Pt 16):2813–2819. [PubMed: 10910765]

Kremer BE, Haystead T, Macara IG. Mammalian septins regulate microtubule stability through interaction with the microtubule-binding protein MAP4. Mol Biol Cell 2005;16:4648–4659. [PubMed: 16093351]

Kudo N, Matsumori N, Taoka H, Fujiwara D, Scheiner EP, Wolff B, Yoshida M, Horinouchi S. Leptomycin B inactivates CRM1/exportin 1 by covalent modification at a cysteine residue in the central conserved region. Proc Natl Acad Sci U S A 1999;96:9112–9117. [PubMed: 10430904]

Kusch J, Meyer A, Snyder MP, Barral Y. Microtubule capture by the cleavage apparatus is required for proper spindle positioning in yeast. Genes Dev 2002;16:1627–1639. [PubMed: 12101122]

Latreille M, Larose L. Nck in a complex containing the catalytic subunit of protein phosphatase 1 regulates eukaryotic initiation factor 2alpha signaling and cell survival to endoplasmic reticulum stress. J Biol Chem 2006;281:26633–26644. [PubMed: 16835242]

Lew DJ. The morphogenesis checkpoint: how yeast cells watch their figures. Curr Opin Cell Biol 2003;15:648–653. [PubMed: 14644188]

Longtine MS, DeMarini DJ, Valencik ML, Al-Awar OS, Fares H, De Virgilio C, Pringle JR. The septins: roles in cytokinesis and other processes. Curr Opin Cell Biol 1996;8:106–119. [PubMed: 8791410]

Longtine MS, Theesfeld CL, McMillan JN, Weaver E, Pringle JR, Lew DJ. Septin-dependent assembly of a cell cycle-regulatory module in Saccharomyces cerevisiae. Mol Cell Biol 2000;20:4049–4061. [PubMed: 10805747]

Low C, Macara IG. Structural analysis of septin 2, 6, and 7 complexes. J Biol Chem 2006;281:30697–30706. [PubMed: 16914550]

Martens N, Uzan G, Wery M, Hooghe R, Hooghe-Peters EL, Gertler A. Suppressor of cytokine signaling 7 inhibits prolactin, growth hormone, and leptin signaling by interacting with STAT5 or STAT3 and attenuating their nuclear translocation. J Biol Chem 2005;280:13817–13823. [PubMed: 15677474]

Martens N, Wery M, Wang P, Braet F, Gertler A, Hooghe R, Vandenhaute J, Hooghe-Peters EL. The suppressor of cytokine signaling (SOCS)-7 interacts with the actin cytoskeleton through vinexin. Exp Cell Res 2004;298:239–248. [PubMed: 15242778]

Martin KH, Slack JK, Boerner SA, Martin CC, Parsons JT. Integrin connections map: to infinity and beyond. Science 2002;296:1652–1653. [PubMed: 12040184]

Matuoka K, Miki H, Takahashi K, Takenawa T. A novel ligand for an SH3 domain of the adaptor protein Nck bears an SH2 domain and nuclear signaling motifs. Biochem Biophys Res Commun 1997;239:488–492. [PubMed: 9344857]

Nagata K, Asano T, Nozawa Y, Inagaki M. Biochemical and cell biological analyses of a mammalian septin complex, Sept7/9b/11. J Biol Chem 2004;279:55895–55904. [PubMed: 15485874]

Nagata K, Inagaki M. Cytoskeletal modification of Rho guanine nucleotide exchange factor activity: identification of a Rho guanine nucleotide exchange factor as a binding partner for Sept9b, a mammalian septin. Oncogene 2005;24:65–76. [PubMed: 15558029]

Oegema K, Savoian MS, Mitchison TJ, Field CM. Functional analysis of a human homologue of the Drosophila actin binding protein anillin suggests a role in cytokinesis. J Cell Biol 2000;150:539–552. [PubMed: 10931866]

Ono R, Ihara M, Nakajima H, Ozaki K, Kataoka-Fujiwara Y, Taki T, Nagata K, Inagaki M, Yoshida N, Kitamura T, et al. Disruption of Sept6, a fusion partner gene of MLL, does not affect ontogeny, leukemogenesis induced by MLL-SEPT6, or phenotype induced by the loss of Sept4. Mol Cell Biol 2005;25:10965–10978. [PubMed: 16314519]

Richards SA, Lounsbury KM, Carey KL, Macara IG. A nuclear export signal is essential for the cytosolic localization of the Ran binding protein, RanBP1. J Cell Biol 1996;134:1157–1168. [PubMed: 8794858]

Sheffield PJ, Oliver CJ, Kremer BE, Sheng S, Shao Z, Macara IG. Borg/septin interactions and the assembly of mammalian septin heterodimers, trimers, and filaments. J Biol Chem 2003;278:3483–3488. [PubMed: 12446710]

Sibani S, Price GB, Zannis-Hadjopoulos M. Decreased origin usage and initiation of DNA replication in haploinsufficient HCT116 Ku80+/− cells. J Cell Sci 2005;118:3247–3261. [PubMed: 16014376]

Smith JA, Poteet-Smith CE, Xu Y, Errington TM, Hecht SM, Lannigan DA. Identification of the first specific inhibitor of p90 ribosomal S6 kinase (RSK) reveals an unexpected role for RSK in cancer cell proliferation. Cancer Res 2005;65:1027–1034. [PubMed: 15705904]

Smolka MB, Chen SH, Maddox PS, Enserink JM, Albuquerque CP, Wei XX, Desai A, Kolodner RD, Zhou H. An FHA domain-mediated protein interaction network of Rad53 reveals its role in polarized cell growth. J Cell Biol 2006;175:743–753. [PubMed: 17130285]

Spiliotis ET, Kinoshita M, Nelson WJ. A mitotic septin scaffold required for Mammalian chomosome congression and segregation. Science 2005;307:1781–1785. [PubMed: 15774761]

Spiliotis ET, Nelson WJ. Here come the septins: novel polymers that coordinate intracellular functions and organization. J Cell Sci 2006;119:4–10. [PubMed: 16371649]

Surka MC, Tsang CW, Trimble WS. The mammalian septin MSF localizes with microtubules and is required for completion of cytokinesis. Mol Biol Cell 2002;13:3532–3545. [PubMed: 12388755]

Vega IE, Hsu SC. The septin protein Nedd5 associates with both the exocyst complex and microtubules and disruption of its GTPase activity promotes aberrant neurite sprouting in PC12 cells. Neuroreport 2003;14:31–37. [PubMed: 12544826]

Xue J, Tsang CW, Gai WP, Malladi CS, Trimble WS, Rostas JA, Robinson PJ. Septin 3 (G-septin) is a developmentally regulated phosphoprotein enriched in presynaptic nerve terminals. J Neurochem 2004;91:579–590. [PubMed: 15485489]

Zhu T, Goh EL, LeRoith D, Lobie PE. Growth hormone stimulates the formation of a multiprotein signaling complex involving p130(Cas) and CrkII. Resultant activation of c-Jun N-terminal kinase/stress-activated protein kinase (JNK/SAPK). J Biol Chem 1998;273:33864–33875. [PubMed: 9837978]

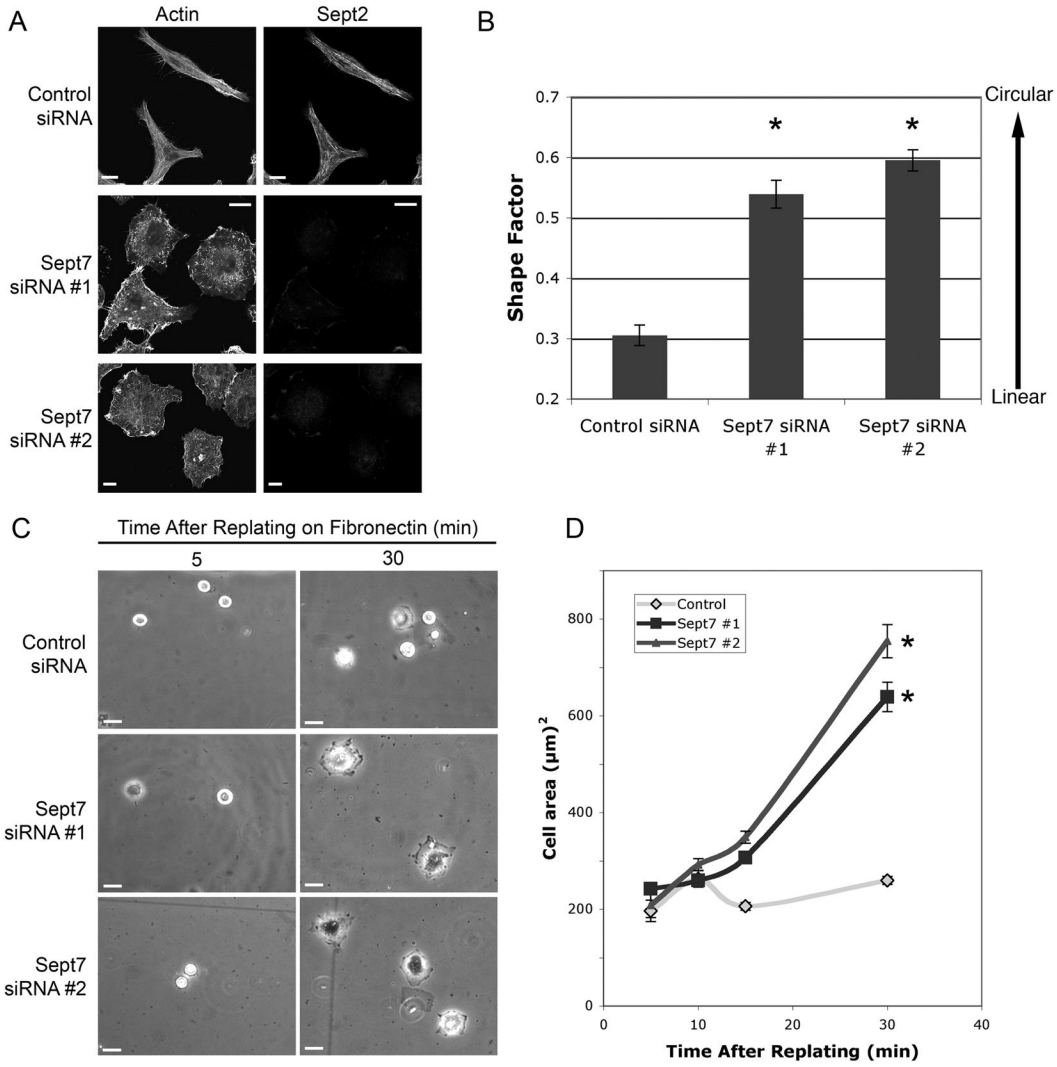

Figure 1. Septin depletion leads to changes in cell morphology, actin cytoskeleton, and cell spreading

(A) Septin knockdown changes cell morphology and actin organization. Control or septin-depleted HeLa cells were fixed and stained with phalloidin and anti-Sept2. Bars=10μm.

(B) Quantification of cell morphology. Areas and perimeters of at least 25 cells from 3 separate experiments were determined. Graph represents the shape factor (SF, $4\pi A/P^2$), ± S.E.M. *: P<0.001 compared to control.

(C) Septin knockdown alters cell spreading on fibronectin. Control- or septin depleted HeLa cells were replated onto fibronectin-coated slides and fixed at 5, 10, 15, and 30 mins; samples of 5 min (left) and 30 min (right) are shown. Bars = 20 μm.

(D) Quantification of cell spreading on fibronectin. Areas of at least 50 cells from 2 separate experiments were calculated for each time point. Bars = S.E.M. *: P<0.001 compared to control at same timepoint.

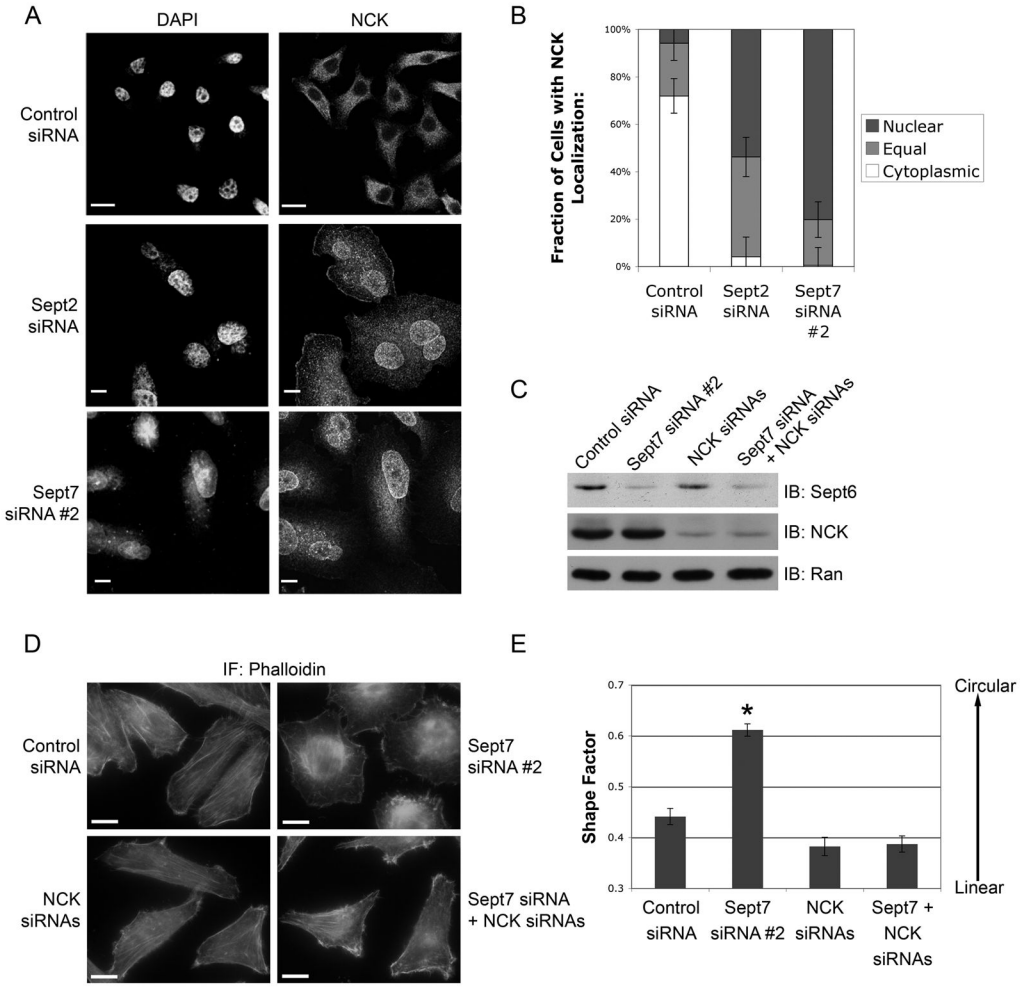

Figure 2. Septin depletion induces nuclear accumulation of the adapter protein NCK, which mediates actin re-organization

(A) Septin depletion induces nuclear accumulation of NCK. Control or septin-depleted HeLa cells were stained with DAPI and mouse anti-NCK and imaged by confocal microscopy. Bars = 10 μm.

(B) Quantification of NCK accumulation. At least 150 cells from 2 separate experiments were imaged randomly and scored for the localization of endogenous NCK. Bars = S.E.

(C) Efficiency of dual septin-NCK depletion. Control-, septin-, NCK-, or septin + NCK siRNA HeLa cells were lysed and blotted for Sept6, NCK, and Ran.

(D) NCK is necessary for effects of septin depletion on cell morphology and the actin cytoskeleton. HeLa cells were fixed and stained with phalloidin to visualize actin and cellular morphology. Bar = 10 μm.

(E) Quantification of effect of double Sept7-NCK depletion on cellular morphology. Shape factors for at least 60 cells from 2 separate experiments were calculated. Bars = S.E.M. *: P<0.001, compared to all other conditions.

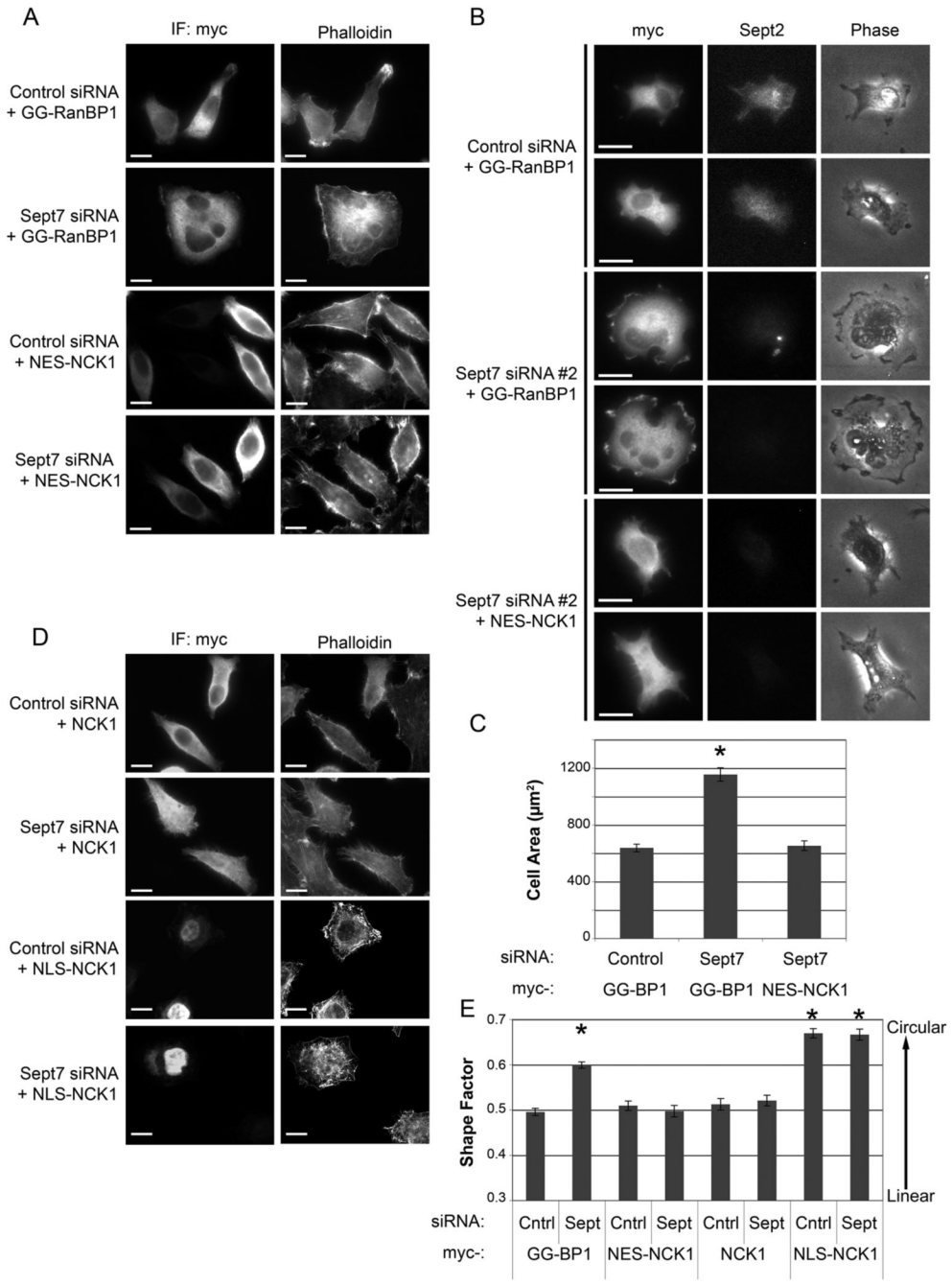

Figure 3. Expression of cytoplasmic NCK is sufficient to reverse septin-mediated phenotypes

(A) Expression of NES-NCK reverses the effects of septin depletion on actin and morphology. Control or septin-depleted HeLa cells were co-transfected with myc-GG-RanBP1 or myc-NES-NCK, as indicated. The cells were fixed and stained with anti-myc antibody and phalloidin. Bar = 10 μm.

(B) Expression of NES-NCK reverses the effects of septin depletion on cellular spreading on fibronectin. Control or septin-depleted HeLa cells were co-transfected with myc-GG-RanBP1 or myc-NES-NCK1, then replated onto a fibronectin-coated substrate, fixed after 30 mins, and stained for myc and Sept2. Random 20X fields were collected for each condition to determine cellular area. Bar = 20 μm.

(C) Quantification of effects of NES-NCK1 expression on cell spreading. The area of at least 75 cells from 2 separate experiments was measured for each condition. *: $P<0.001$, compared to other conditions. Bars = S.E.M.

(D) Cytoplasmic NCK is essential for normal morphology. Control or septin-depleted HeLa cells were co-transfected with myc-NCK1 or myc-NLS-NCK1, fixed, and stained for myc and actin. Bar = 10 μm.

(E) Quantification of effects of NCK localization on cellular shape. Random fields were collected from 3 separate experiments, and the shape factors for at least 150 cells per condition were calculated. Bars = S.E.M. *: $P<0.001$, compared to NES-NCK1, myc-NCK1, and control siRNA + GG-BP1-transfected cells.

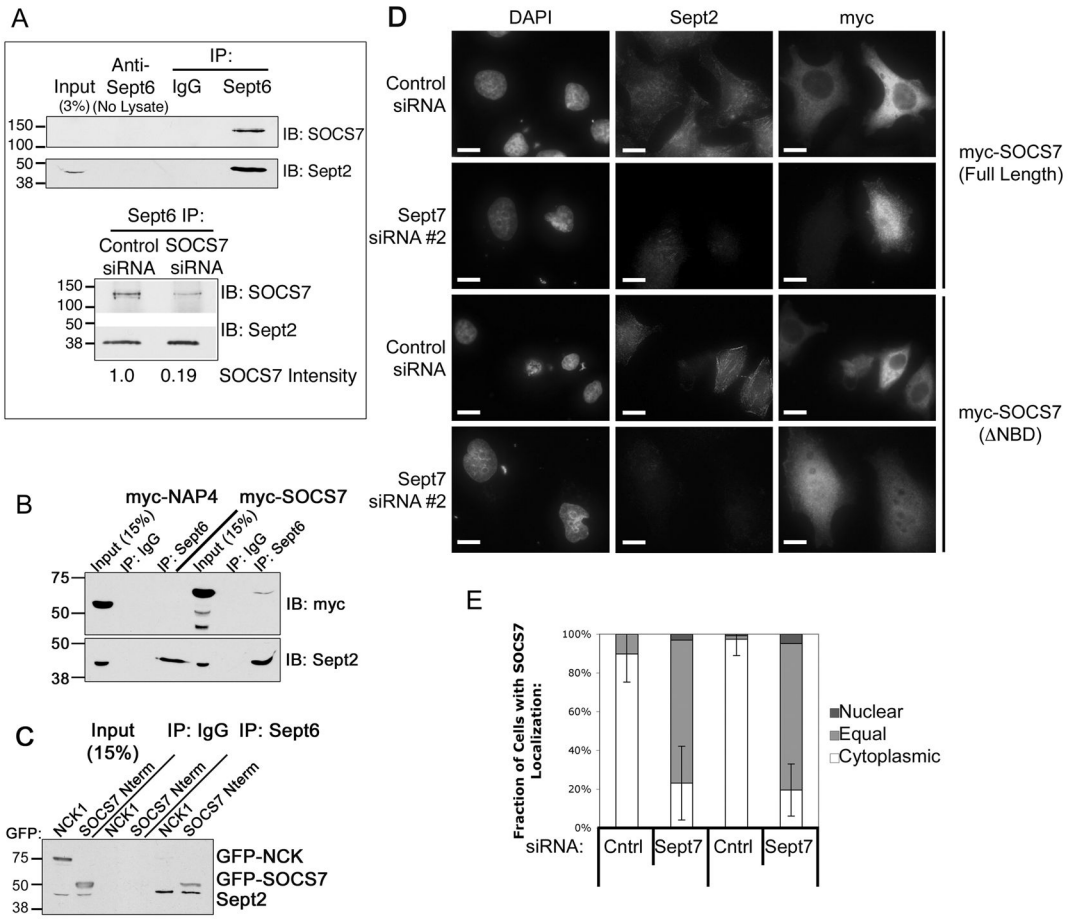

Figure 4. The role of SOCS7 in the septin-depletion phenotype

(A) Septins interact with endogenous SOCS7. (Top) Endogenous Sept6 was immunoprecipitated from HeLa cell lysate, and the precipitates were probed for endogenous SOCS7 and Sept2. (Bottom) Endogenous Sept6 was precipitated from control- and SOCS7-depleted HeLa cells to confirm identity of the SOCS7 protein.

(B) Septins interact with longer-variant SOCS7, but not with the splice variant NAP4. HEK 293T cells were transfected with myc-tagged NAP4 or SOCS7. Endogenous Sept6 was immunoprecipitated and probed with anti-myc and anti-Sept2.

(C) Sept6 interacts with the N-terminal region of SOCS7. GFP-tagged NCK or SOCS7 Nterm (aa 1-124) were transfected into HEK 293T cells, and endogenous Sept6 was immunoprecipitated. Top: Anti-GFP immunoblot. Bottom: Anti-Sept2 immunoblot.

(D) Septin depletion induces nuclear accumulation of SOCS7. Control- or septin-depleted cells were co-transfected with myc-SOCS7, fixed, and stained with DAPI, anti-Sept2, and anti-myc. Full length SOCS7 (top two rows) or a variant lacking the NCK binding domain (ΔNBD, bottom two rows) were used. Bar = 10 μm.

(E) Quantification of SOCS7 localization. At least 70 transfected cells in 2 separate experiments for each condition were scored for SOCS7 localization. Bars = S.E.

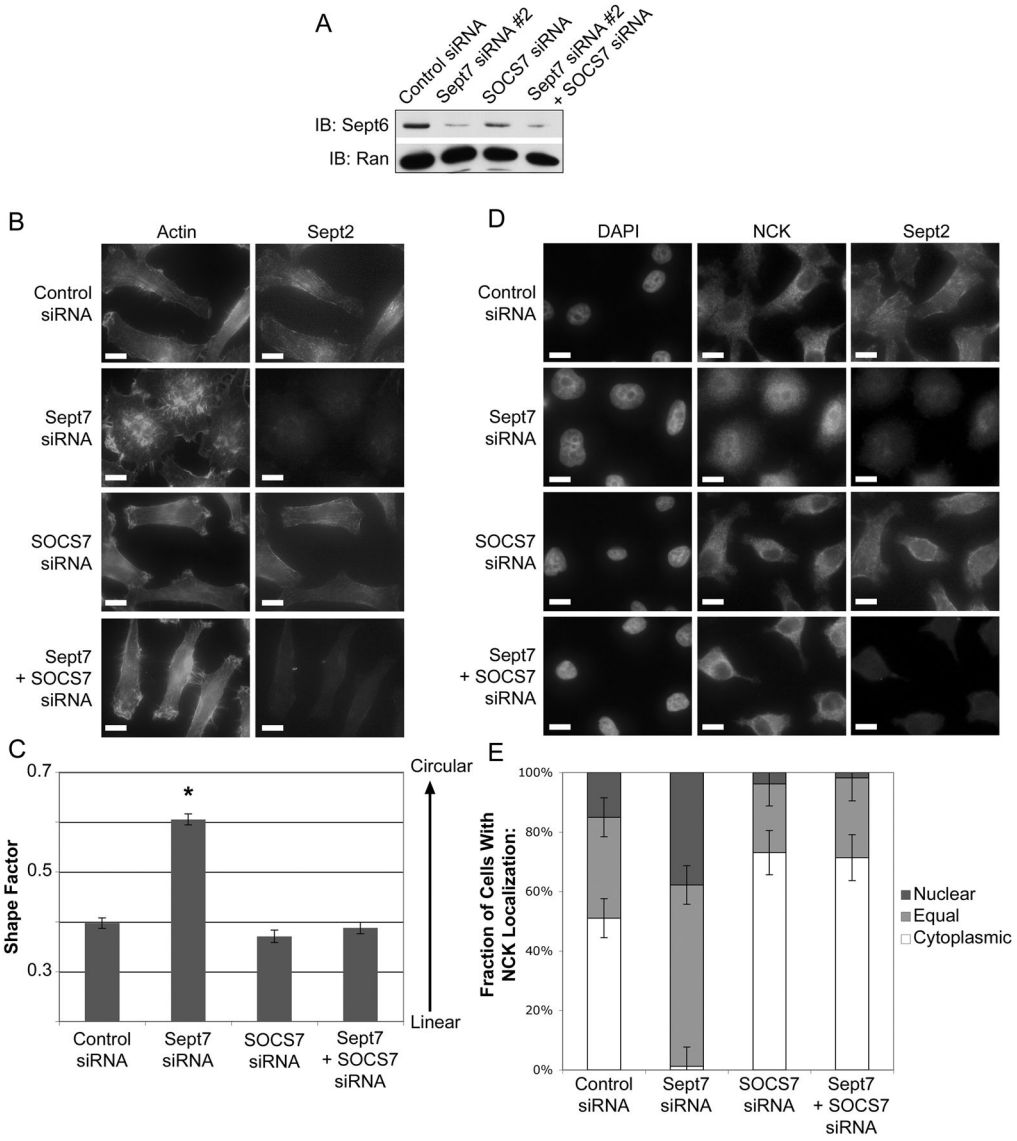

Figure 5. SOCS7 is necessary for septin loss-of-function phenotype

(A) Septin knockdown is equally efficient for single septin knockdown and septin-SOCS7 knockdown. HeLa cells were transfected as indicated, lysed, then blotted for Sept6 (top) and Ran (bottom).

(B) SOCS7 depletion reverses effects of septin knockdown on morphology and the actin cytoskeleton. HeLa cells were transfected as indicated, fixed, and stained for actin and Sept2. Bar = 10 μm.

(C) Quantification of cell morphology. The shape factors of at least 100 cells from 2 separate experiments were determined. Bars = S.E.M. *: P<0.001, compared to all other conditions.

(D) Loss of SOCS7 prevents NCK relocalization in septin-depleted cells. HeLa cells were transfected as indicated, then fixed and stained with DAPI, anti-NCK, and anti-Sept2. Bar = 10 μm.

(E) NCK relocalization depends on SOCS7. NCK localization was determined as described above for at least 100 cells in 2 experiments. Bars = S.E.

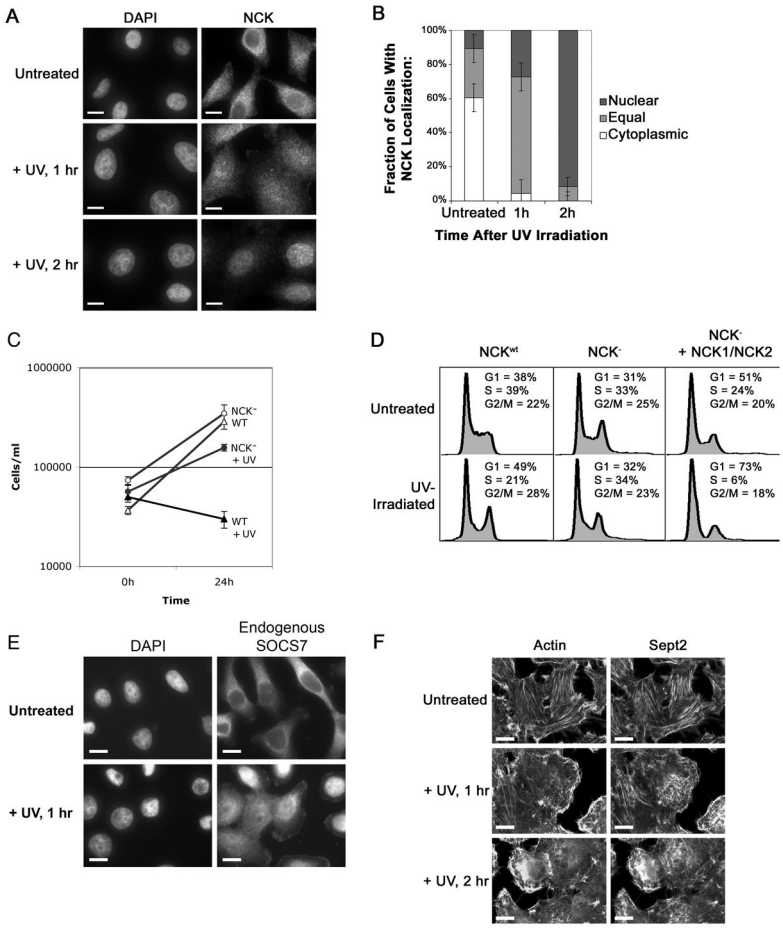

Figure 6. NCK relocalizes to the nucleus in response to DNA damage, and is necessary for DNA damage-induced cell cycle arrest

(A) NCK accumulates in the nucleus following UV irradiation. HeLa cells were UV-irradiated, incubated in growth medium for the times indicated, then fixed and stained with DAPI and anti-NCK. Bar = 10 μm.

(B) Quantitation of UV-induced NCK relocalization. At least 100 cells from 2 separate experiments were scored for NCK localization. Bars = S.E.

(C) NCK is necessary for UV-induced cell cycle arrest. NCK^{wt} and NCK−/− cells were UV irradiated, then lifted and counted 0h and 24h after irradiation. A representative triplicate experiment is shown. Bars = S.E.M.

(D) NCK is necessary for UV-induced cell cycle arrest. NCK^{wt} or NCK−/− cells were UV-irradiated, cultured for 29h, then lifted and PI-stained for cell cycle analysis. To verify rescue, NCK−/− cells were transfected with myc-tagged NCK1 and NCK2, then irradiated and stained as described in Experimental Procedures. Cells with an anti-myc intensity of 10^2 and greater (~6–7% of the total population) were selected for cell cycle analysis. Values shown are the mean of at least 3 experiments per condition.

(E) SOCS7 enters the nucleus after UV irradiation. HeLa cells were UV-irradiated, fixed, and stained with DAPI and anti-SOCS7. Bar = 10 μm.

(F) UV irradiation disrupts septin filaments and actin stress fibers. HeLa cells were UV-irradiated, grown for the times indicated, then fixed and stained for actin and Sept2. Bar = 10 μm.

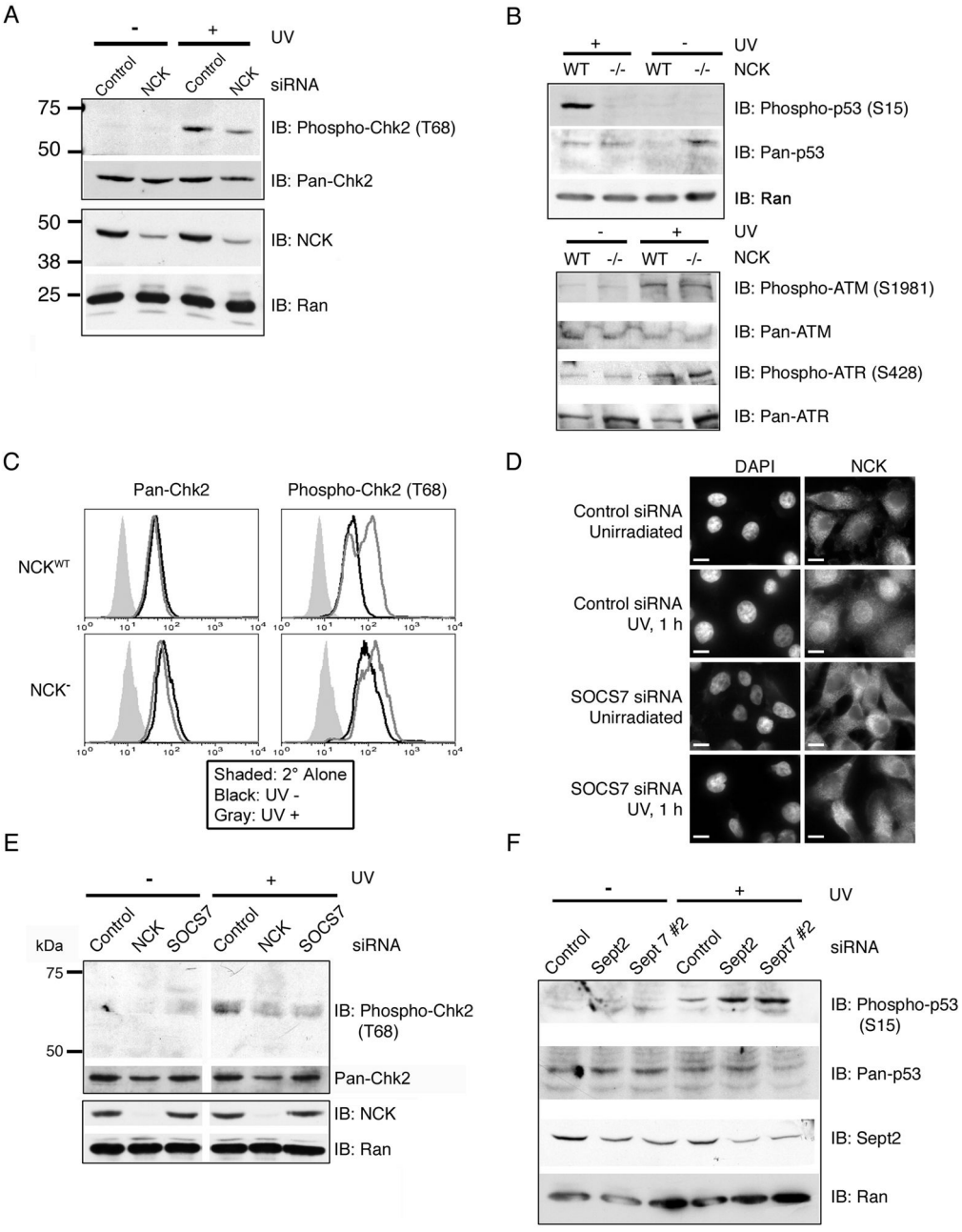

Figure 7. Nuclear transport of NCK is necessary for activation of the DNA damage cascade

(A) NCK is necessary for full activation of Chk2. Control- or NCK-depleted HeLa cells were UV-irradiated, lysed, and probed for activated and total Chk2.

(B) NCK is necessary for phosphorylation of p53. NCK^{wt} and NCK−/− MEFs were UV irradiated, lysed, and probed for activated and total p53, ATM, and ATR, and for total Ran.

(C) NCK is necessary for full activation of Chk2. NCK^{wt} and NCK−/− MEFs were UV irradiated and analyzed for total or phosphorylated (T68) Chk2 by flow cytometry. Panels are representative of 3 independent experiments. X-axis: fluorescence intensity, Y-axis: frequency as a percentage of total cells.

(D) SOCS7 transports NCK into the nucleus in response to UV. Control- or SOCS7-siRNA cells were UV irradiated, fixed, and stained with DAPI and anti-NCK. Bar = 10 μm.
(E) Nuclear transport of NCK is necessary for full activation of Chk2. Control-, NCK, or SOCS7-depleted cells were UV irradiated, lysed, and probed with antibodies against phospho-Chk2 (Th68), pan-Chk2, NCK, and Ran.
(F) Septins regulate DNA damage response. Control-, Sept2-, and Sept7-siRNA transfected MEF^{wt} were UV irradiated, lysed, and probed with anti-phospho-p53 (Ser15), total p53, -Sept2, and Ran.